DR. ABDELHALIM AZZI (Orcid ID : 0000-0003-2429-2100)

Received Date : 21-Apr-2020

Revised Date : 09-Aug-2020

Accepted Date : 26-Aug-2020

Article type : Research Article

SHIP2 inhibition alters redox-induced PI3K/AKT and MAP kinase pathways via PTEN over-activation in cervical cancer cells

Abdelhalim Azzi[1]

[1] GIGA-Molecular Biology of Disease, GIGA-B34, University of Liège, Liège, Belgium

Corresponding author:

This article has been accepted for publication and undergone full peer review but has not been through the copyediting, typesetting, pagination and proofreading process, which may lead to differences between this version and the Version of Record. Please cite this article as doi: 10.1002/2211-5463.12967

Abdelhalim Azzi, GIGA-Molecular Biology of Disease, GIGA-B34, Centre Hospitalier Universitaire Sart-Tilman, Université de Liège, avenue de l'Hôpital 11, 4000-Liège, Belgium. Email: halim1904@gmail.com.

Running heading: SHIP2 inhibition in cervical cancer

Abbreviations: SHIP2: SH2-domain containing phosphatidylinositol-3,4,5-trisphosphate 5-phosphatase 2, PI3K: phosphoinositide 3-kinase; AKT: Protein kinase B; MAPK: mitogen activated protein kinase; PtdIns(3,4,5)P3: phosphatidylinositol 3,4,5-trisphosphate; PtdIns(4,5)P2: phosphatidylinositol 4,5-bisphosphate; ERK: extracellular signal–regulated kinases; PTEN: phosphatase and tensin homologue.

Abstract

PI(3,4,5)P3 is required for AKT activation. The level of PI(3,4,5)P3 is constantly regulated through balanced synthesis by PI3 kinase and degradation by phosphoinositide phosphatases PTEN and SHIP2, known as negative regulators of AKT. Here, I show that SHIP2 inhibition in cervical cancer cell lines alters H_2O_2-mediated AKT and MAPK/ERK pathway activation. In addition, SHIP2 inhibition enhances reactive oxygen species generation. Interestingly, I found that SHIP2 inhibition and H_2O_2 treatment enhance lipid and protein phosphatase activity of PTEN. Pharmacological targeting or RNAi-mediated knockdown of PTEN rescue ERK and AKT activation. Using a series of pharmacological and biochemical approaches, I provide evidence that crosstalk between SHIP2 and PTEN occurs upon an increase in oxidative stress to modulate the activity of MAPK and PI3/ATK pathways.

Keywords: SHIP2, PTEN, SHIP2 inhibitor, ROS, PI3K/Akt pathway.

1. Introduction

Reactive oxygen species (ROS) play a central role in cellular physiology [1-2]. At lower concentration, they play a role as a second messenger by regulating diverse aspects of cellular signaling during organismal development [3-4]. However, at high concentration, ROS alter cellular function by damaging lipids, proteins and DNA leading to the activation of stress signaling pathways. Activation of these pathways leads to growth arrest to repair damages and promote survival, or activates cell death [5-7]. Hydrogen peroxide (H_2O_2) is the main substance used to study oxidative stress at the cellular level. Experimental evidence exists for H_2O_2 mediated ROS production that activates several signaling pathways, among which mitogen-activated protein kinase (MAPK) and phosphatidylinositol 3-kinase (PI3-kinase)/ protein kinase B (PKB/Akt), which promote cell growth and survival [8-9]. Activation of the MAP kinase family members, extracellular signal-regulated kinases 1 and 2 (ERK1/2), block apoptosis in response to H_2O_2 [10]. The anti-apoptotic effect of ERK1/2 for example, involves protection against caspase activation and loss of mitochondrial membrane potential [11-12]. In addition to MAP Kinase, AKT activation also blocks apoptosis and enhances survival in response to exogenous H_2O_2. The anti-apoptotic effect of AKT involves direct phosphorylation and inactivation of pro-apoptotic proteins [13-15]. Activation of AKT requires PI(3,4,5)P3 [16]. Intracellular levels of PI(3,4,5)P3 is constantly regulated by a balance of two processes that involve synthesis by PI3 Kinase and

degradation by phosphoinositide phosphatases PTEN and SHIP2 [15, 17]. PTEN (phosphatase and tensin homologue) dephosphorylates the 3-position phosphate of PI(3,4,5)P3 and PI(3,4)P2 to generate respectively PI(4,5)P2 and PI4P, and this event results in suppression of AKT signaling [18]. The SH2-domain containing phosphatidylinositol-3,4,5-trisphosphate 5-phosphatase 2, or SHIP2, dephosphorylates the 5-position phosphate from PI(3,4,5)P3 to generate PI(3,4)P2 leading also to inhibition of AKT mediated signaling pathways in response to growth factor like insulin [19-20]. Previous studies have shown that SHIP2 plays a role in regulation of PI3K-dependent insulin signaling [21-23]. Further to its role as a lipid phosphatase, SHIP2 plays also a role as a scaffolding protein in other aspects of signaling, including cell migration, adhesion, and endocytosis [24-26]. Interestingly, recent findings reported that dysregulation in the levels of SHIP2 protein alters cellular health and signaling. For example, overexpression of SHIP2 suppresses AKT activation and promotes apoptosis, while its knockdown enhance AKT activation and promotes cell growth [27-28]. Moreover, SHIP2 is also involved in oxidative stress-activated signaling. Overexpression of the dominant-negative form of SHIP2 in hepatocellular carcinoma cells HepG2, suppresses palmitate induced apoptosis, enhances AKT activation and reduces ROS generation [29]. However, this study was performed in cells that express lower levels of PTEN. So far, signaling crosstalk between SHIP2 and PTEN in response to oxidative stress has not been a subject of investigation. Here, I used a pharmacological approach to examine whether blocking SHIP2 would promote AKT activation and survival upon H_2O_2-induced oxidative stress in cervical cancer cell lines. Experiments were carried out in HeLa and SiHa cells, which express higher levels of both SHIP2 and PTEN [30-31]. SHIP2 was blocked using the 3-[(4-chlorobenzyl)oxy]-N-[(1S)-1-phenylethyl]-2-thiophene-carboxamide (AS1949490), a small molecule drug that was previously characterized from a high-throughput screen [32]. The specificity of the inhibitory activity of AS1949490 was validated *in vitro* as well as *in vivo* [32-33]. In this study, I report that in response to H_2O_2, SHIP2 inhibition enhances lipid and protein phosphatase activity of PTEN which in turn downregulates MAP Kinase and PI3 kinase/Akt pathways.

2. Results

2.1. Catalytic inhibition of SHIP2 alters PI3 Kinase and MAP kinase activation in stimuli and cell type dependent manner

Cervical cancer cell lines express high levels of SHIP2 and PTEN [30-31] (**Figure 1a** and **Sup. Figure 1**). To test whether SHIP2 plays a role in signaling upon an increase in levels of reactive oxygen species (ROS), HeLa cells were treated with a vehicle or SHIP2 inhibitor AS1938909 (abbreviated as AS19) [32]. 24 hours later, cells were stimulated with 1 mM H_2O_2 for 1 hour. As a readout of PI3 Kinase and MAP kinase activation, AKT phosphorylation at Ser473 and ERK1/2 phosphorylation known to be activated by H_2O_2 were used to examine these pathways [8-9]. Western blot analysis showed that in vehicle treated cells, H_2O_2 induces phosphorylation of both AKT and ERK proteins (**Figure 1b**). Unexpectedly, cells in which SHIP2 was inhibited, phosphorylation of both proteins were less pronounced. To further confirm the inhibitory activity of AS19 [32-33], I first analyzed its effect in response to other stimuli in HeLa cells. As indicated in **Figure 1c**, upon growth factor stimulation, AS19 mediated SHIP2 inhibition induces sustained activation of AKT, demonstrating that the chemical inhibitor indeed blocks the lipid phosphatase activity of SHIP2. Next, I examined the effect of AS19 in another cell line, human embryonic kidney HEK293T cells. As shown in **Figure 1d,** SHIP2 inhibition did not suppress AKT phosphorylation upon H_2O_2 treatment. Moreover, SHIP2 inhibition enhances both basal and H_2O_2 induced ERK1/2 phosphorylation. Together, these results show that the difference of activation of the two signaling pathways upon SHIP2 inhibition is both stimuli and cell type dependent. Then I focused on the molecular mechanism that drive this difference in signaling in HeLa cells.

I first examined whether lower AKT and ERK1/2 phosphorylation seen upon SHIP2 inhibition and H_2O_2 stimulation is time dependent. Compared to vehicle treated cell, longer treatment with H_2O_2 did not increase AKT and ERK phosphorylation upon SHIP2 inhibition (**Figure 1e**). In addition to these differences in H_2O_2 signalling response, PARP cleavage, known as a marker of apoptosis was also analysed [34]. Contrary to previous observation [29], SHIP2

inhibition did not prevent oxidative stress induced apoptosis (**Figure 1e**). To further confirm that SHIP2 inhibition induces apoptosis in these cells, mitochondrial membrane potential (ΔΨm) was verified. ROS-mediated apoptosis alters mitochondrial dynamics as well as mitochondrial membrane potential (ΔΨm) [35]. I therefore examined whether SHIP2 inhibition alters mitochondrial properties. MitoTracker Red CMXRos, a fluorescent dye that accumulates specifically in intact mitochondria was used [36]. Under basal conditions, SHIP2 inhibition has no effect on ΔΨm. However, upon H_2O_2 treatment, cells in which SHIP2 is inactivated exhibited a marked drop in the mitochondrial membrane potential, indicative of apoptosis activation (**Figure 1f-g**).

2.2. SHIP2 inhibition alters AKT and ERK phosphorylation through increase in ROS generation

Previous studies have shown that SHIP2 inhibition lead to lower ROS production in response to diverse stimuli including palmitate and high glucose [29, 37]. To examine whether the effect of SHIP2 inhibition on AKT and ERK activation is mediated through ROS production, the fluorescent probe DCFDA was used to monitor ROS levels in HeLa cells under different conditions. While basal ROS were not different, SHIP2 inhibition in these cells generates significantly higher ROS upon H_2O_2 treatment (**Figure 2a**). Next, to investigate whether SHIP2 inhibition mediated lower ERK and AKT phosphorylation observed above is due to high increase in ROS levels, pyruvate was used as a ROS scavenger [38]. As indicated in **Figure 2b**, pre-treatment of cells with 5 mM pyruvate led to significant reduction in ROS production. In addition, lowering ROS level re-activated both AKT and ERK phosphorylation and prevented H_2O_2 induced cell death (**Figure 2c-d**). Taken together, these demonstrated that SHIP2 inhibition alters ROS production upon H_2O_2 treatment. Although, less pronounced, similar effects were observed in another cervical cancer cell line, SiHa. Indeed, SHIP2 inhibition in these cells induces lower activation of PI3K/AKT pathway. Moreover, consistent with the results seen in HeLa cells, pyruvate pre-treatment lead to marked increase in AKT phosphorylation (See **Sup. Figure 2a-c**).

2.3. SHIP2 inhibition induces overactivation of PTEN upon increase of ROS

The role of SHIP2 as a negative regulator of the PI3K/AKT is very well established [19, 23]. For example, upon insulin stimulation, SHIP2 localizes to the plasma membrane to negatively regulate AKT phosphorylation [39]. Contrary to growth factor stimulation [24, 39], fluorescence imaging of GFP-SHIP2 dynamics showed that H_2O_2 treatment induces clustering of the protein with minor localization to the plasma membrane. Similar clustering and localization were seen in cells treated with the catalytic inhibitor following H_2O_2 treatment (**Sup. Figure 3a**). It is likely that SHIP2 plays different function in response to hydrogen peroxide. The fact that SHIP2 inhibition induces lower activation of AKT suggests alteration in either PI (3,4,5)P3 synthesis or degradation. To test this hypothesis, I first examined levels of PI (3,4,5)P3 under different conditions. Cells transfected with GFP-PH-BTK plasmid construct were used. This strategy is based on the use of specific protein domain e.g., PH-BTK that bind phosphoinositides. When fused to GFP, dynamic changes in phosphoinositides can be visualized *in vitro* [40]. GFP-PH-BTK reporter was used to visualize the PI (3,4,5)P3 in control and SHIP2 inhibited cells. Consistent with AKT phosphorylation levels, 1 h of H_2O_2 stimulation led to marked accumulation of PI (3,4,5)P3 at the plasma membrane in control cells, whereas very low levels of PI (3,4,5)P3 were seen in cells in which SHIP2 was inhibited (**Figure 3a**). Consistent with previous findings, PI (3,4,5)P3 accumulation was supressed upon PI3 Kinase inhibitor, wortmannin [41]. In addition, the kinetics of ERK and AKT activation upon H_2O_2 stimulation was dramatically different. H_2O_2 treatment leads to marked increase and sustained phosphorylation of both proteins in control cells, whereas only minor phosphorylation of AKT and ERK was seen in SHIP2-inhibited cells which then decreased over time (**Figure 3b**). Next, I used AKT activator, SC79 a known PI (3,4,5)P3 mimetics that binds the pleckstrin homology (PH) domain of AKT and enhances its phosphorylation [42]. As indicated in **Figure 3c**, SC79 rescues AKT phosphorylation in cells in which SHIP2 was inactivated. However, this increase occurred only at early time points. Upon 4 h of H_2O_2 treatment, SC79 treatment led

to a constant increase in AKT phosphorylation in control cells, whereas no marked change was seen in SHIP2 inhibited cells (**Sup. Figure 3b**).

PTEN (phosphatase and tensin homolog) negatively regulates levels of PI (3,4,5)P3 in different contexts and function as a tumor suppressor by suppressing AKT signaling pathway [17-18]. Previous studies have shown that ROS simultaneously activates PI3 kinase and inactivates PTEN via oxidation of cysteine residues within the active site of the protein [43-44]. Based on our observation that SHIP2 inhibition alters levels of PI (3,4,5)P3 and kinetic activation of AKT, phosphorylation of PTEN at residues Ser380 known as a negative marker of PTEN activity was analyzed [45]. As indicated in **Figure 3d-e** and contrary to vehicle-treated cells, SHIP2 inhibition markedly enhance PTEN activity as shown by dramatic decrease in PTEN phosphorylation upon H_2O_2 treatment. Together, these experiments demonstrated that SHIP2 inhibition enhances PTEN activation upon H_2O_2 treatment which might negatively affect AKT and ERK phosphorylation.

2.4. PTEN inhibition rescue mitochondrial membrane potential loss and lowers ROS generation

Previous findings have shown that ROS triggers localization of PTEN to mitochondria [46]. Further, it is reported that a fraction of PTEN localizes to the endoplasmic reticulum (ER) and mitochondria-associated membranes (MAMs) to modulate intracellular calcium (Ca^{2+}) release from the ER to mitochondria in response to apoptotic stimuli [47]. Therefore, I examined the effect of simultaneous inhibition of SHIP2 and PTEN on mitochondrial properties. The percentage of cells displaying positive staining for MitoTracker Red were measured. As shown in (**Figure 4 a-b**), PTEN inhibition led to significant increase in proportion of intact mitochondria specifically in cells in which SHIP2 was inactivated. PTEN inhibition affected not only ($\Delta\Psi m$) but also mitochondria morphology. Simultaneous inhibition of PTEN and SHIP2 induced perinuclear aggregate of hyper fused mitochondria. Although is not examined here, it should be noted that two very recent studies reported that the long isoform of PTEN plays a role in mitophagy, a process that involves selective degradation of

mitochondria by autophagy [48-49]. In addition, PTEN inhibition moderately lowered ROS production upon H_2O_2 treatment in cells in which SHIP2 was blocked (**Figure 4c**).

2.5. PTEN inhibition rescue ERK activation

To mechanistically understand the impact of PTEN overactivation induced by SHIP2 inhibition and ROS accumulation. I first examined the lipid phosphatase activity of PTEN. Given that PI (3, 4)P2 also known as a major substrate for PTEN, and is required for full activation of AKT [50-51], I used GFP-PH-TAPP1 reporter to visualize the PI (3, 4)P2 in control and SHIP2 inactivated cells. One hour of H_2O_2 treatment led to marked cellular accumulation of PI (3,4)P2 in control cells, whereas very low levels of PI (3,4)P2 was seen in cells in which SHIP2 was inhibited (**Figure 5a**). Interestingly, PTEN inhibition and H_2O_2 treatment led to a substantial increase of PI (3,4)P2 in control cells. However, only moderate accumulation of PI (3,4)P2 was seen in cells treated with SHIP2 and PTEN inhibitors following H_2O_2 treatments. Next, I analysed the effect of change in PTEN activity on ERK and AKT phosphorylation upon 4 h H_2O_2 treatment. Western blot analysis showed that pre-treatment of control cells with PTEN inhibitor significantly increased phosphorylation of both ERK and AKT. Surprisingly, in SHIP2-inactivated cells, PTEN inhibition had only minor effect on AKT phosphorylation but rather rescued MAP kinase activation, as indicated by a significant increase in ERK phosphorylation (**Figure 5b-c**). To further ascertain that PTEN inhibition has only a minor effect on AKT phosphorylation in SHIP2-inhibited cells, I analysed kinetic activation of ERK and AKT upon simultaneous H_2O_2 treatment and PTEN inhibition at earlier time points. PTEN inhibition led to substantial increase in ERK phosphorylation in all conditions. However, when compared to control cells, increase in AKT phosphorylation upon simultaneous SHIP2 and PTEN inhibition was only seen at 30 min following H_2O_2 treatment (**Figure 5d**). I conclude that SHIP2 inhibition induces constitutive activation of PTEN upon the increase of ROS, and that both lipid and protein phosphatase of PTEN might be affected.

2.6. SHIP2 inhibition alters both lipid and protein phosphatase activity of PTEN

The results above showed that chemical inhibition of PTEN rescued only MAP kinase activation and mitochondrial membrane potential, suggesting that overactivation of PTEN seen upon SHIP2 inhibition could also involve its protein phosphatase activity. Indeed, in addition to its lipid phosphatase activity, previous reports have shown that PTEN is able to dephosphorylate the isoform p52Shc of SHC-transforming protein 1, leading to downregulation of the Ras-ERK pathway activity [52-53]. Therefore, I examined p52Shc phosphorylation dynamics under different conditions. As indicated in **Figure 6a**, SHIP2 inhibition reduces both basal and H_2O_2 induced p52Shc phosphorylation. Interestingly, PTEN inhibition increased phosphorylation of both ERK and p52Shc, further indicating that SHIP2 inhibition enhances both lipid and protein phosphatase activity of PTEN upon H_2O_2 treatment. These findings were further validated by siRNA mediated knockdown of PTEN. Indeed, reduced PTEN protein level induces lower ERK phosphorylation in both conditions while rescuing AKT phosphorylation in SHIP2 inhibited cells (**Figure 6b**). Altogether, these findings demonstrated that in cervical cancer cell lines, SHIP2 inhibition and H_2O_2 induced ROS generation enhances both lipid and protein phosphatase activity of PTEN which in turn downregulates MAP Kinase and PI3 kinase/Akt pathways.

3. Discussion

Reactive oxygen species (ROS) plays a crucial role during organismal development. At lower concentrations, they are involved in activating diverse signaling pathways leading to cell growth and differentiation. At high levels, or dysregulation in cellular redox balances, ROS induces oxidative stress [1-2]. Dysregulation in redox balance has been implicated in a various pathophysiological condition including cancer, neurodegeneration, and alteration in the immune system [54]. Oxidative stress induces inflammation and causes cell death by apoptosis or necrosis [6-7]. Recent studies have highlighted the role of SHIP2 in modulating cellular signaling pathways in response to different stressors. As a negative regulator of PI(3,4,5)P3 level, SHIP2 inhibition in liver cancer cells enhance PI3K/AKT signaling and prevents ROS production following palmitate treatment [29], whereas its overexpression supresses PI3K/AKT signaling and cell growth in in gastric cancer cells [27]. SHIP2 and PTEN are the major negative regulator of PI3K/AKT signaling [18-20], and both proteins are highly expressed in cervical cancer cell lines HeLa and Siha (**Figure 1a** and **Sup. Figure 1**). In this study, I provide the first evidence that SHIP2 inhibition in these cells induces PETN activation upon H_2O_2 treatment, which in turn alter MAP kinase and PI3K/AKT signaling pathways. Moreover, and contrary to previous findings in liver cancer cell line [29], SHIP2 inhibition in cervical cancer cell lines enhances ROS production, a common consequence of oxidative stress-mediated cell death. In this regard, ROS scavenger pyruvate, reactivated PI3K/AKT signaling and prevented H_2O_2 induced cell death (**Figure 2b-d**).

Our data suggest that SHIP2 plays different function in cell-type and stimuli-dependent manner. Indeed, growth factor stimulation enhances AKT phosphorylation; whereas, H_2O_2 attenuates AKT phosphorylation upon SHIP2 inactivation (**Figure 1b-c**). The role of SHIP2 as a lipid phosphatase in response to growth factor is very well established. It accumulates at the plasma membrane and modulates PI3 kinase downstream signaling through its lipid phosphatase activity [23, 39], whereas H_2O_2 treatment induces clustering of the protein with minor localization to the plasma membrane (**Sup. Figure S3a**), demonstrating stimuli-dependent dynamics of SHIP2.

Together, our results at least in cervical cancer cells establish a concept that whereas in response to growth factors SHIP2 localize to the plasma membrane and prevent sustained activation of both PI3K/Akt and MAP Kinase through its lipid phosphatase activity. However, in response to H_2O_2, it is likely that SHIP2 plays a role as scaffolding protein to maintain sustained activation of PI3K/Akt and MAP Kinase. Consistently, lipid phosphates independent roles of SHIP2 in signal transduction have been reported recently. Indeed, in human embryonic kidney cells, HEK293T, loss of SHIP2 alters ERK activation in response to fibroblast growth factor (FGF) stimulation [55]. In accordance with these findings, our observations suggest that the inhibitor might not only block the catalytic activity of SHIP2 but also its scaffolding function by altering SHIP2 interaction with its partners. Therefore, a comprehensive study would be needed to clarify how this chemical inhibitor affects SHIP2 structural conformation and its interaction with other proteins.

One of the most interesting findings in the present study is that SHIP2 inhibition induces overactivation of PTEN upon H_2O_2 treatment, which in turn lowers level of PI (3,4,5)P3 and PI (3,4)P2 and suppresses AKT activation. Surprisingly, while chemical inhibition of PTEN rescue ERK phosphorylation no marked change in AKT phosphorylation was seen (**Figure 5b-c**). These results suggest activation of both lipid and protein phosphates of PTEN upon SHIP2 inhibition. Indeed, in addition to its lipid phosphatase, PTEN possess a protein phosphatase activity. For example, Gu *et al.* demonstrated that PTEN dephosphorylates Src homology 2 domain-containing protein (SHC) and suppresses ERK activation [53]. Consistent with these findings, PTEN inhibition enhance p52Shc phosphorylation (**Figure 6a**). To further examine the role of PTEN protein upon SHIP2 inhibition, I used siRNA knockdown. I could provide evidence that downregulation of PTEN rescued AKT phosphorylation upon SHIP2 inhibition (**Figure 6b**). It should be noted that PTEN was not fully abolished by siRNA and the remaining protein might be sufficient to block overactivation of AKT upon SHIP2 inhibition. Altogether the results presented here highlight a crosstalk between SHIP2 and PTEN. The mechanistic crosstalk was not examined. However, two possibility might explain PTEN overactivation. One possibility is that increase in PI(4,5)P2 upon SHIP2 inhibition (**Sup. Figure 4**) might enhance PTEN phosphatase activity. Indeed,

PI (4,5)P2 is known as a cofactor that binds PTEN and enhances its lipid phosphatase activity [56]. Alternatively, or in addition to the first possibility, structural changes of SHIP2 upon binding to AS1938909 releases SHC which then can be dephosphorylated by PTEN. Indeed, SHIP2 and PTEN also modulate MAP and PI3 Kinase activity upon binding to SHC [39, 53]. The signaling mechanism that drive PTEN overactivation upon SHIP2 inhibition is beyond the scope of the current study, but in future studies, it would be important to reveal the mechanistic crosstalk between these two proteins particularly in cancer development. Indeed, SHIP2 is involved in regulation of several cellular processes like adhesion and migration, which are known hallmarks of cancer progression and metastasis [24-26]. In this regard Hoekstra et al., reported that SHIP2 is highly expressed in colorectal cancer tissue [57]. Consistent with our observations, SHIP2 inhibition in colorectal cancer cells reduces AKT phosphorylation [57]. Altogether, these findings suggest that SHIP2 might play a role in cancer development and progression, providing a new potential therapeutic target.

4. Materials and Methods

4.1. Reagents

Dulbecco's Modified Eagle Medium (DMEM) was purchased from Gibco Cat. No 41966052 (Fisher scientific), SHIP2 Inhibitor AS1938909 Cat. No SML1022 (Sigma). Hydrogen peroxide (Sigma). PTEN inhibitor VO-Ohpic trihydrate Cat. No. S8174 (Selleckchem), 2′,7′-Dichlorofluorescin diacetate Cat. No D6883 (Sigma), 3-Methyladenine Cat. No M9281 (Sigma), MitoTracker® Red CMXRos Cat. No 9082 (Cell signaling), 4′,6-diamidino-2-phenylindole dihydrochloride (DAPI) were purchased from Molecular Probes (Life Technologies, Carlsbad, CA).

4.2. Cell culture

HEK293T and HeLa cells were obtained from Prof. Stéphane Schurmans (GIGA- Laboratory of Functional Genetics, University of Liege). SiHa cells were obtained from Dr. Shostak Kateryna (GIGA-University of Liege).

Cells were grown as recommended in DMEM containing 4.5 g/L d-Glucose supplemented with 10% fetal bovine serum (FBS), 100 U/mL penicillin, 100 U/mL streptomycin and 1% L-glutamine (Gibco). Cells between three and ten passages were used. All cultures were maintained at 37 °C in a humidified 5% CO2 incubator. Unless otherwise stated, cell were treated with 10 μM SHIP2 inhibitor AS1949490 or equivalent volume of DMSO as a control for 24 h.

4.3. Determination of ROS levels

Cytoplasmic ROS levels were measured using the fluorescent probe 2′,7′-Dichlorofluorescin diacetate (DCFDA) in a final concentration of 25 μM. Cells were seeded overnight at equal density, 15000 cells per well in a 96-well plate. Upon 24 h treatment with DMSO as vehicle or SHIP2 inhibitor (10 μM), DCFDA was supplemented to the growth medium and incubated for 30 min at 37 °C. Stained cells were rinsed with warm basal DMEM and incubated again

for 1h in fresh medium. Where indicated pyruvate pretreatment (5 mM) for 1h followed by H_2O_2 (1 mM). Fluorescent signal detection was measured using Tecan Infinite M200 PRO Multi-Detection Microplate Reader (Tecan Life science) or VICTOR™ X Series Multilabel Plate Readers (PerkinElmer) set to 485 nm excitation and 530 nm emission wavelength.

4.4. Immunofluorescence

Cell were plated overnight on glass coverslips in 24-well plates (150,000 cells/well) followed by treatment with vehicle or SHIP2 inhibitor for 24 h. For mitochondria staining, live cells were supplemented with 100 nM MitoTracker® Red for 30 min at 37 °C. Upon different treatments, cells were fixed using ice cold methanol at -20°C during 10 minutes. Upon three-time washes with PBS cells were then incubated with DAPI (0.1 µg/ml). Images were captured using Leica TCS SP5 microscope and processed with ImageJ (NIH).

4.5. siRNA transfections

siRNA transfection was performed using Dharmafect 4 according to manufacturer instruction (Dharmacon). Briefly cells were plated a day before at 50% confluence. They were then transfected with 75 nM siRNA. Twenty four hours later medium was replaced, then treated with vehicle or SHIP2 inhibitor for 24 h where indicated. The following siRNA were used, ON-TARGET plus SMART pool siRNA against PTEN (#L003023-00-0005) and a control siRNA (#D-001810-10-05).

4.6. Plasmid transfection:

Plasmid transfection was performed using lipofectamine 3000 according to manufacturer instructions. The following plasmids construct GFP-SHIP2, GFP-BTK-PH, GFP- TAPP1-PH and GFP-PLCδ-PH were obtained from Prof. Stéphane Schurmans (GIGA- Laboratory of Functional Genetics, University of Liege).

4.7. Western blotting

Cells were first washed with PBS and then resuspended in RIPA buffer (150 mM NaCl, 1.0% NP-40, 0.5% sodium deoxycholate, 0.1% SDS, 50 mM Tris-HCl, pH 8.0), containing protease and phosphatase inhibitors (ROCHE). Protein samples were collected by centrifugation (10000xG, 10 min) at 4°C. Sample concentrations were quantified using Biorad Protein Assay according to manufacturer instructions. Equal amounts of protein

extract were loaded and separated by SDS-PAGE and then transferred to nitrocellulose membranes. The membranes were blocked for 60 min at room temperature with 5% Bovine serum albumin in Tris-buffered saline supplemented with 0.05 % Tween 20 (TBST). Membranes were then incubated with primary antibodies overnight at 4 °C, followed by HRP-labeled secondary antibodies. Labeled proteins were visualized with an enhanced chemiluminescence system (Fisher scientific). Optical densities of proteins were determined using ImageJ.

The following antibodies were all purchased from Cell signaling (phospho-AKT S473 #4060, AKT #4691, phospho-ERK (Thr202/Tyr204) #4377, ERK #4695, PARP #9542, Phospho-MEK1/2 (Ser217/221) #9121, MEK1/2 #9122, phosphor-Pten S380 #9551, Pten #5959, vinculin #13901 and phospho-SHC (Tyr239/240) #2434). Horseradish peroxidase (HRP)-linked secondary antibodies, Rabbit A0545 and Mouse A9044 from Sigma. Actin and SHC from Santa Cruz Biotechnology, respectively SC-1616 and SC-967. Anti-SHIP2 gift from Prof. Christophe Erneux (IRIBHM, Université Libre de Bruxelles, Belgium).

4.8. Cell viability

Cell viability was measured using Cell Counting Kit-8 (CCK-8) Cat. No 96992 (Sigma). Cells were first seeded overnight at equal density, 15000 cells per well in a 96-well plate. They were then treated with vehicle or SHIP2 inhibitor for 24 h followed by 1 mM H_2O_2 for 4 h and treated with WST-8 for 1 h at 37 °C. The absorbance at 450 nm was then measured using Tecan Infinite M200 PRO Multi-Detection Microplate Reader.

Mitochondrial membrane potential measurement

Mitochondrial membrane potential measurement was performed using Cell Meter™ Mitochondrion Membrane Potential Assay Kit (AAT Bioquest #22805). HeLa cells were seeded overnight at equal density, 10,000 cells per well in a 96-well plates, then treated with vehicle or 10µM SHIP2 inhibitor for 24 hours. Upon 1mM H_2O_2 treatment during 90 minutes, MitoTell™ Orange solution was added and incubated 30 minutes at 37°C. Assay Buffer B was then added. Fluorescence was then measured using Infinite M200 PRO Multi-Detection Microplate Reader. Excitation wavelength was set at 540 nm and emission wavelength at

590 nm. Quantification was performed relative to control untreated cells. HeLa cells treated with Carbonyl cyanide m-chlorophenyl hydrazone CCCP 20μM (ab141229, abcam) were used as a control.

4.9. Statistical analysis

Statistical analyses were performed using GraphPad Prism 7 Software (GraphPad Software, San Diego, CA). Data were presented as mean±S.D. For comparisons of three or more conditions, one-way analysis of variance with Tukey's HSD post hoc test was used. Differences with less than 0.05 were considered statistically significant.

Acknowledgements

This work was supported by the Swiss National Science Foundation (SNSF) grant ID (P2ZHP3_162156) and Marie Skłodowska-Curie Actions and University of Liège (COFUD-2015). I would like to thank Prof. Stéphane Schurmans for accepting me as a visiting scientist in his laboratory and for providing space and reagents necessary to perform experiments. I also would like to thank Prof. C. Erneux for providing us SHIP2 antibody, Dr. Charles-Andrew Vande Catsyne, Dr. Bastien Moes, Dr. Dayana Abboud, Dr. Martin Alexander Lopez, Aurore Cué-Alvarez and Monique Henket for their support and GIGA imaging platform for their technical support. Dr. Jihwan Myung (Taipei Medical University) for the insightful discussion.

Conflicts of Interest: The author declare no conflict of interest.

Data accessibility: The raw data of this study are available from the corresponding author on reasonable request.

Author contributions:

AA conceived and designed the experiments; AA acquired, analyzed and interpreted the data and wrote the manuscript.

References

1 Circu ML and TY Aw (2010) Reactive oxygen species, cellular redox systems, and apoptosis. Free Radic Biol Med **48**: 749–62.

2 Zorov DB, M Juhaszova and SJ Sollott (2006) Mitochondrial ROS-induced ROS release: an update and review. Biochim Biophys Acta **1757**: 509–17.

3 Irani K (2000) Oxidant signaling in vascular cell growth, death, and survival: a review of the roles of reactive oxygen species in smooth muscle and endothelial cell mitogenic and apoptotic signaling. Circ Res **87**: 179–83.

4 Perez-Vizcaino F, A Cogolludo and L Moreno (2010) Reactive oxygen species signaling in pulmonary vascular smooth muscle. Respir Physiol Neurobiol **174**: 212–20.

5 Flohé L (2010) Changing paradigms in thiology from antioxidant defense toward redox regulation. Methods Enzymol **473**:1–39.

6 Ott M, Vladimir Gogvadze, Sten Orrenius, Boris Zhivotovsky (2007) Mitochondria, oxidative stress and cell death. Apoptosis **12**: 913–22.

7 Stefan W Ryter, Hong Pyo Kim, Alexander Hoetzel, Jeong W Park, Kiichi Nakahira, Xue Wang, Augustine M K Choi (2007) Mechanisms of cell death in oxidative stress. Antioxid Redox Signal **9**:49–89.

8 Mohamad Z Mehdi, Nihar R Pandey, Sanjay K Pandey, Ashok K Srivastava (2005) H2O2-induced phosphorylation of ERK1/2 and PKB requires tyrosine kinase activity of insulin receptor and c-Src. Antioxid Redox Signal **7**:1014–20.

9 Azar ZM, MZ Mehdi and AK Srivastava (2006) Activation of insulin-like growth factor type-1 receptor is required for H2O2-induced PKB phosphorylation in vascular smooth muscle cells. Can J Physiol Pharmacol **84**:777–86.

10 X Wang, J L Martindale, Y Liu and N J Holbrook (1998) The cellular response to oxidative stress: influences of mitogen-activated protein kinase signalling pathways on cell survival. Biochem J **333**:291–300.

11 Erhardt P, EJ Schremser and GM Cooper (1999) B-Raf inhibits programmed cell death downstream of cytochrome c release from mitochondria by activating the MEK/Erk pathway. Mol Cell Biol **19**:5308–15.

12 T Shonai, M Adachi, K Sakata, M Takekawa, T Endo, K Imai, M Hareyama (2002) MEK/ERK pathway protects ionizing radiation-induced loss of mitochondrial membrane potential and cell death in lymphocytic leukemia cells. Cell Death Differ **9**:963–71.

13 Sung-Wuk Jang, Seung-Ju Yang, Shanthi Srinivasan, Keqiang Ye (2007) Akt phosphorylates MstI and prevents its proteolytic activation, blocking FOXO3 phosphorylation and nuclear translocation. J Biol Chem **282**:30836–44.

14 Song G, G Ouyang and S Bao (2005) The activation of Akt/PKB signaling pathway and cell survival. J Cell Mol Med **9**:59–71.

15 Manning BD and LC Cantley (2007) AKT/PKB signaling: navigating downstream. Cell **129**:1261–74.

16 Mehdi MZ, ZM Azar and AK Srivastava (2007) Role of receptor and nonreceptor protein tyrosine kinases in H2O2-induced PKB and ERK1/2 signaling. Cell Biochem Biophys **47**:1–10.

17 Takehiko Sasaki, Shunsuke Takasuga, Junko Sasaki, Satoshi Kofuji, Satoshi Eguchi, Masakazu Yamazaki, Akira Suzuki (2009) Mammalian phosphoinositide kinases and phosphatases. Prog Lipid Res **48**:307–43.

18 Leslie NR and CP Downes (2002) PTEN: The down side of PI 3-kinase signalling. Cell Signal **14**:285–95.

19 Christophe Erneux, William's Elong Edimo, Laurence Deneubourg, Isabelle Pirson (2011) SHIP2 multiple functions: a balance between a negative control of PtdIns(3,4,5)P_3 level, a positive control of PtdIns(3,4)P_2 production, and intrinsic docking properties. J Cell Biochem **112**:2203–9.

20 Saqib U and MI Siddiqi (2011) Insights into structure and function of SHIP2-SH2: homology modeling, docking, and molecular dynamics study. J Chem Biol **4**:149–58.

21 S Clément, U Krause, F Desmedt, J F Tanti, J Behrends, X Pesesse, T Sasaki, J

Penninger, M Doherty, W Malaisse, J E Dumont, Y Le Marchand-Brustel, C Erneux, L Hue, S Schurmans (2001) The lipid phosphatase SHIP2 controls insulin sensitivity. Nature **409**:92–7.

22 Kazuhito Fukui, Tsutomu Wada, Syota Kagawa, Kiyofumi Nagira, Mariko Ikubo, Hajime Ishihara, Masashi Kobayashi, Toshiyasu Sasaoka (2005) Impact of the liver-specific expression of SHIP2 (SH2-containing inositol 5'-phosphatase 2) on insulin signaling and glucose metabolism in mice. Diabetes **54**:1958–67.

23 D Blero, F De Smedt, X Pesesse, N Paternotte, C Moreau, B Payrastre, C Erneux (2001) The SH2 domain containing inositol 5-phosphatase SHIP2 controls phosphatidylinositol 3,4,5-trisphosphate levels in CHO-IR cells stimulated by insulin. Biochem Biophys Res Commun **282**:839–43.

24 Laura Chan Wah Hak, Shaheen Khan, Ilaria Di Meglio, Ah-Lai Law, Safa Lucken-Ardjomande Häsler, Leonor M Quintaneiro, Antonio P A Ferreira, Matthias Krause, Harvey T McMahon, Emmanuel Boucrot (2018) FBP17 and CIP4 recruit SHIP2 and lamellipodin to prime the plasma membrane for fast endophilin-mediated endocytosis. Nat Cell Biol **20**:1023–1031.

25 William's Elong Edimo, Ana Raquel Ramos, Somadri Ghosh, Jean-Marie Vanderwinden, Christophe Erneux (2016) The SHIP2 interactor Myo1c is required for cell migration in 1321 N1 glioblastoma cells. Biochem Biophys Res Commun **476**: 508–514.

26 Prasad NK and SJ Decker (2005) SH2-containing 5'-inositol phosphatase, SHIP2, regulates cytoskeleton organization and ligand-dependent down-regulation of the epidermal growth factor receptor. J Biol Chem **280**:13129–36.

27 Yan Ye, Yan Mei Ge, Miao Miao Xiao, Li Mei Guo, Qun Li, Ji Qing Hao, Jie Da, Wang Lai Hu, Xu Dong Zhang, Jiegou Xu, Lin Jie Zhang (2016) Suppression of SHIP2 contributes to tumorigenesis and proliferation of gastric cancer cells via activation of Akt. J Gastroenterol **51**:230–40.

28 Mervi E Hyvönen, Pauliina Saurus, Anita Wasik, Eija Heikkilä, Marika Havana, Ras Trokovic, Moin Saleem, Harry Holthöfer, Sanna Lehtonen (2010) Lipid phosphatase

SHIP2 downregulates insulin signalling in podocytes. Mol Cell Endocrinol **328**:70–9.

29 Gorgani-Firuzjaee S, K Adeli and R Meshkani (2015) Inhibition of SH2-domain-containing inositol 5-phosphatase (SHIP2) ameliorates palmitate induced-apoptosis through regulating Akt/FOXO1 pathway and ROS production in HepG2 cells. Biochem Biophys Res Commun **464**:441–6.

30 Uhlen M et al. (2017) A pathology atlas of the human cancer transcriptome. Science **357**(6352).

31 Human Protein Atlas available from www.proteinatlas.org

32 A Suwa, T Yamamoto, A Sawada, K Minoura, N Hosogai, A Tahara, T Kurama, T Shimokawa and I Aramori (2009) Discovery and functional characterization of a novel small molecule inhibitor of the intracellular phosphatase, SHIP2. Br J Pharmacol **158**:879–87.

33 Liu SL et al. (2018) Quantitative Lipid Imaging Reveals a New Signaling Function of Phosphatidylinositol-3,4-Bisphophate: Isoform- and Site-Specific Activation of Akt. Mol Cell **71**:1092–1104.

34 Chaitanya GV, AJ Steven and PP Babu (2012) PARP-1 cleavage fragments: signatures of cell-death proteases in neurodegeneration. Cell Commun Signal **8**: 31.

35 Marchi S et al. (2012) Mitochondria-ros crosstalk in the control of cell death and aging. J Signal Transduct **2012**:329635.

36 Pendergrass W, N Wolf and M Poot (2004) Efficacy of MitoTracker Green and CMXrosamine to measure changes in mitochondrial membrane potentials in living cells and tissues. Cytometry A **61**:162–9.

37 Gorgani-Firuzjaee S and R Meshkani (2015) SH2 domain-containing inositol 5-phosphatase (SHIP2) inhibition ameliorates high glucose-induced de-novo lipogenesis and VLDL production through regulating AMPK/mTOR/SREBP1 pathway and ROS production in HepG2 cells. Free Radic Biol Med **89**:679–89.

38 Xiaofei Wang, Evelyn Perez, Ran Liu, Liang-Jun Yan, Robert T Mallet and Shao-Hua Yang (2007) Pyruvate protects mitochondria from oxidative stress in human neuroblastoma SK-N-SH cells. Brain Res **1132**:1–9.

39 Hajime Ishihara, Toshiyasu Sasaoka, Manabu Ishiki, Tsutomu Wada, Hiroyuki Hori, Syota Kagawa, Masashi Kobayashi (2002) Membrane localization of Src homology 2-containing inositol 5'-phosphatase 2 via Shc association is required for the negative regulation of insulin signaling in Rat1 fibroblasts overexpressing insulin receptors. Mol Endocrinol **16**:2371–81.

40 Balla T and P Várnai (2016) Visualization of cellular phosphoinositide pools with GFP-fused protein-domains. Curr Protoc Cell Biol, Chapter 24: p. Unit 24.4.

41 William's Elong Edimo, Somadri Ghosh, Rita Derua, Veerle Janssens, Etienne Waelkens, Jean-Marie Vanderwinden, Pierre Robe, Christophe Erneux (2016) SHIP2 controls plasma membrane PI(4,5)P2 thereby participating in the control of cell migration in 1321 N1 glioblastoma cells. J Cell Sci **129**:1101–14.

42 Jo H et al. (2012) Small molecule-induced cytosolic activation of protein kinase Akt rescues ischemia-elicited neuronal death. Proc Natl Acad Sci U S A **109**:10581–6.

43 Seung-Rock Lee, Kap-Seok Yang, Jaeyul Kwon, Chunghee Lee, Woojin Jeong and Sue Goo Rhee (2002) Reversible inactivation of the tumor suppressor PTEN by H2O2. J Biol Chem **277**:20336–42.

44 Jaeyul Kwon, Seung-Rock Lee, Kap-Seok Yang, Younghee Ahn, Yeun Ju Kim, Earl R Stadtman and Sue Goo Rhee (2004) Reversible oxidation and inactivation of the tumor suppressor PTEN in cells stimulated with peptide growth factors. Proc Natl Acad Sci U S A **101**:16419–24.

45 Benjamin D Hopkins, Cindy Hodakoski, Douglas Barrows, Sarah M Mense, Ramon E Parsons (2014) PTEN function: the long and the short of it. Trends Biochem Sci **39**:183–90.

46 Zhu Y, Hoell P, Ahlemeyer B, Krieglstein J (2006) PTEN: a crucial mediator of mitochondria-dependent apoptosis. Apoptosis **11**:197–207.

47. A Bononi, M Bonora, S Marchi, S Missiroli, F Poletti, C Giorgi, P P Pandolfi and P Pinton (2013) Identification of PTEN at the ER and MAMs and its regulation of Ca(2+) signaling and apoptosis in a protein phosphatase-dependent manner. Cell Death Differ **20**:1631–43.

48 Wang L et al. (2018) PTEN-L is a novel protein phosphatase for ubiquitin dephosphorylation to inhibit PINK1-Parkin-mediated mitophagy. Cell Res **28**:787–802.

49 Guoliang Li, Jingyi Yang, Chunyuan Yang, Minglu Zhu, Yan Jin, Michael A McNutt and Yuxin Yin (2018) PTENα regulates mitophagy and maintains mitochondrial quality control. Autophagy **14**:1742–1760.

50 Malek M et al. (2017) PTEN Regulates PI(3,4)P2 Signaling Downstream of Class I PI3K. Mol Cell **68**:566–580.

51 Scheid MP et al. (2002) Phosphatidylinositol (3,4,5)P3 is essential but not sufficient for protein kinase B (PKB) activation; phosphatidylinositol (3,4)P2 is required for PKB phosphorylation at Ser-473: studies using cells from SH2-containing inositol-5-phosphatase knockout mice. J Biol Chem 277:9027–35.

52 Jianguo Gu, Masahito Tamura, Roumen Pankov, Erik HJ Danen, Takahisa Takino, Kazue Matsumoto, Kenneth M Yamada (1999) Shc and FAK differentially regulate cell motility and directionality modulated by PTEN. J Cell Biol **146**:389–403.

53 Gu J, M Tamura and KM Yamada (1998) Tumor suppressor PTEN inhibits integrin- and growth factor-mediated mitogen-activated protein (MAP) kinase signaling pathways. J Cell Biol **143**:1375–83.

54 Ilaria Liguori, Gennaro Russo, Francesco Curcio et al. (2018) Oxidative stress, aging, and diseases. Clin Interv Aging **13**:757–772.

55 Bohumil Fafilek, Lukas Balek, Michaela Kunova Bosakova et al. (2018) The inositol phosphatase SHIP2 enables sustained ERK activation downstream of FGF receptors by recruiting Src kinases. Sci Signal, **11**(548).

56 Campbell RB, F Liu and AH Ross (2003) Allosteric activation of PTEN phosphatase by phosphatidylinositol 4,5-bisphosphate. J Biol Chem **278**:33617–20.

57 Elmer Hoekstra, Asha M Das, Marcella Willemsen et al. Lipid phosphatase SHIP2 functions as oncogene in colorectal cancer by regulating PKB activation. Oncotarget **7**:73525–73540.

Figure legends

Figure 1. SHIP2 inhibition alters the PI3K and MAPkinase pathways upon H2O2 treatment. (**a**) Lysates from HepG2 and HeLa cells blotted with the indicated antibodies. Results are representative of two experimental replicates. (**b**) HeLa cells treated with vehicle or SHIP2 inhibitor AS1938909 (AS19) for 24 h then followed by 1 mM H_2O_2 for 30 minute or 1hour. H2O2 treatment was performed in two biological replicates for each condition. Lysates were separated using SDS-PAGE and blotted with the indicated antibodies. Results are representative of two independent experiments. (**c**) HeLa cells treated or not with SHIP2 inhibitor for 24 h followed by 6 h serum starvation (SS), then 10% serum stimulation for the indicated times. (**d**) H_2O_2 induced AKT and ERK1/2 phosphorylation upon SHIP2 inhibition is cell type dependent. HEK293T cells treated with vehicle or AS19 for 24hours then followed by 1 mM H_2O_2 for the indicated times. (**e**) HeLa cells were treated as in (b), then exposed to 4 h H_2O_2 (1 mM). H_2O_2 treatment was performed in two biological replicates for each condition. (**f**) HeLa cells were treated as described in (b), then exposed to 3.5 h H_2O_2 (1 mM). Live cells were stained with 100 nM Mito-tracker red for mitochondria for 30 min then fixed and mounted. Nuclei are stained with DAPI (blue), Mitochondria (red). Scale bar: 10 µM. (**g**) SHIP2 inhibition alters mitochondrial membrane potential. Bar graph showing relative MitoLite fluorescence intensity in each condition following 1mM H_2O_2 treatment during 90 minutes. HeLa cells treated with CCCP alone used as positive control (25µM). Data represent the means ± SEM of 3 independent experiments. One-way ANOVA, $F(3, 60) = 111$, $P<0.0001$. Tukey's multiple comparisons test (*, $p<0.05$, **, $p<0.01$). (C-) vehicle treated cells.

Figure2. SHIP2 inhibition enhances ROS production upon H2O2 treatment.
(**a**) Levels of cytoplasmic ROS in HeLa cells were measured by monitoring DCF fluorescence intensity, H_2O_2 (1 mM). Bar graph summarizing the DCF intensities for each

group, expressed as a fold change relative to control untreated cells. Data are the means ± SEM from 3 independent experiments. One way ANOVA, F(3, 28) =48.13. Tukey's multiple comparisons test. (*, $p<0.05$). (C-) vehicle treated cells. (**b**) Levels of cytoplasmic ROS were measured by monitoring DCF fluorescence intensity. HeLa cells were first treated with vehicle or SHIP2 inhibitor for 24 h followed by pyruvate (5 mM) for 2 h then treated with 1 mM H_2O_2 for 1 h. Bar graph summarizing the DCF intensities for each condition. Data are the means ± SEM from 3 independent experiments. One-way ANOVA, F(5,90)=221, $p<0.0001$. Tukey's multiple comparisons test. (*, $p<0.05$; **, $p<0.01$). (**c**) HeLa cells were treated as described in (a). Lysates were analyzed for the indicated antibodies. (**d**) The ROS scavenger pyruvate prevents hydrogen peroxide induced cell death. Cell viability was measured with CCK-8 assays. HeLa cells were treated as in (a). After 4 h of 1 mM H_2O_2, cells were then treated with WST-8 for 1 h at 37 °C. Data are the means ± SEM from 3 independent experiments. One-way ANOVA, F(5, 66)=812.4, $p<0.0001$. Tukey's multiple comparisons test. (**, $p<0.01$).

Figure3. SHIP inhibition alters PI(3,4,5)P3 levels upon H2O2 stimulation. (**a**) HeLa cells were first transfected with plasmid GFP-tagged BTK-PH domain, 6 h later they were treated with vehicle or AS19 for 24 h. Subsequently cells were treated with 1 mM H_2O_2 for 1 h, then fixed and mounted. Fluorescent images representing PI(3,4,5) P3 levels are shown. Cells pre-treated with 200 nM wortmannin (Wort) used as a control. Arrows indicate PI(3,4,5) P3 signal. Upper and lower panel pictures are from two biological replicates for each condition. Scale bar: 10 μM. (**b**) Kinetic of AKT and ERK phosphorylation in HeLa cells after 24 h of SHIP2 inhibition and subsequent H_2O_2 treatment (1 mM). Lysate collected and analyzed for the indicated times. Short and long exposure for p-AKT and p-ERK were shown. (**c**) HeLa cells were treated with a vehicle or AS19 for 24 h followed by AKT activator (SC79), 20 μM for 2 h then 1 mM H_2O_2 then collected at the indicated times. Short and long exposure of the blots were shown. (**d**) SHIP2 inhibition activates PTEN upon increase in ROS. HeLa cells were treated with vehicle or AS19 for 24 h then followed by 1 mM H_2O_2 for 4 h. Lysates were analyzed for the indicated antibodies. H_2O_2 treatment was performed in three biological replicates for each condition. (**e**) Bar graph summarizing PTEN phosphorylation levels in

HeLa cells for each treatment. Data are the means ± SEM from 3 independent experiments. One way ANOVA, F(3,8)=11.91, p=0.0025. Tukey's multiple comparisons test. (**, p<0.01). (C-) vehicle treated cells.

Figure 4. PTEN inhibition partially rescue mitochondrial membrane potential.

(**a**) HeLa cells were treated with vehicle or AS19 for 24 h then followed by PTEN inhibitor, 2 μM for 2 h then 1 mM H_2O_2 for 3.5h. Live cells were stained with 100 nM Mito-tracker red for mitochondria during 30min then fixed and mounted. Nuclei are stained with DAPI (blue), Mitochondria (red). Scale bar: 10 μM. (**b**) Bar graph summarizing the percentage of mitotracker positive cells under different conditions. Data are the means±SEM from 3 independent experiments. One way ANOVA, F(5,73)=19.54, p<0.0001. Tukey's multiple comparisons test. (**, p<0.01). (**c**) PTEN inhibition reduces ROS production. Bar graph summarizing the DCF intensities for each condition. Data are the means±SEM from 3 independent experiments. One way ANOVA, F(5,174)=749.2, p<0.0001. Tukey's multiple comparisons test. (*, p<0.05). ns: not significant. (C-) vehicle treated cells.

Figure 5. Catalytic inhibition of PTEN rescue PI(3,4)P2 levels and ERK phosphorylation. (**a**) HeLa cells were first transfected with GFP-tagged TAPP1-PH domain plasmid, 6 h later they were treated overnight with vehicle or AS19 followed by 1 mM H_2O_2 for 1 h. Cells were then fixed and mounted. Fluorescent images of PI(3,4) P2 levels are shown. Cells pre-treated with 2 μM PTEN inhibitor (VO-OHpic) were used as a control. Arrows indicate PI(3,4) P2 signal. Scale bar: 10 μM. (**b**) PTEN inhibition rescue MAPkinase activation. HeLa cells treated with vehicle or AS19 for 24 h followed by 2 μM PTEN inhibitor for 2 h then 1 mM H_2O_2 for 4 h. Cell lysates were analyzed for the indicated antibodies. (**c**) Bar graph summarizing ERK and AKT phosphorylation levels for each treatment. Data are the means ± SEM from 3 independent experiments, each in duplicates. p-ERK/ERK, One way ANOVA, F(5,12)=101.1, p<0.0001. Tukey's multiple comparisons test. (**, p<0.01). p-AKT/AKT, One-way ANOVA, F(5, 12)=8.468. (**d**) Catalytic inhibition of PTEN partially rescue AKT phosphorylation only at the early time point. HeLa cells were treated as in (b), then collected at the indicated times. (C-) vehicle treated cells.

Figure 6. SHIP2 inhibition alters both lipid and protein phosphatase activity of PTEN. (**a**) PTEN inhibition activates SHC. HeLa cells were treated with vehicle or AS19 for 24 h followed by PTEN inhibitor (2 μM) during 2h and 1 mM H_2O_2 for 4h. Lysate were blotted for the indicated antibodies. Representative image of two independent experiments. (**b**) PTEN knockdown rescue AKT phosphorylation. HeLa cells were transfected with siRNA control or siRNA directed to PTEN. 24 h later they were treated with vehicle or SHIP2 inhibitor for 24h then followed by 1 mM H_2O_2 during 4 h. Lysate were analyzed for the indicated antibodies. Representative image of two independent experiments.

Supplementary materials.

Supporting file 1: Original uncropped western blots figures. Some pictures are with additional samples data. However, these samples are not related to results of the present manuscript (please see where indicated).

Figure S1. (**a-b**) RNA levels of SHIP2 and PTEN in different cell lines [30-31]. See also: https://www.proteinatlas.org/ENSG00000165458-INPPL1/cell, and https://www.proteinatlas.org/ENSG00000171862-PTEN/cell.

Figure S2. SHIP2 inhibition alters AKT activation upon H2O2 treatment in SiHa cells. (**a**) SiHa cells were first treated with vehicle or SHIP2 inhibitor for 48 h then followed by 1 mM H_2O_2 for 6h. Cell lysates were analyzed for the indicated antibodies. H_2O_2 treatment was performed in biological triplicates for vehicle and SHIP2 inhibited cells. (**b**) The ROS scavenger pyruvate, prevents H_2O_2 induced cell death. SiHa cells were first treated with vehicle or SHIP2 inhibitor for 48 h then followed by pyruvate (5 mM) for 2 h then treated with 1 mM H_2O_2 for 4h. Cell lysates were analyzed for the indicated antibodies. (**c**) SiHa cells were treated as in (b), then cell viability was measured with CCK-8 assays. After 5 h of 1 mM H_2O_2 cells were treated with WST-8 for 1 h at 37 °C. The absorbance at 450 nm was

measured with a microplate reader. Data are the means ± SEM from 2 independent experiments. Each in four replicates. One-way ANOVA, F(5, 62)=92.1, $p<0.0001$. Tukey's multiple comparisons test. (**, $p<0.01$).

Figure S3. H2O2 induces SHIP2 clusters formation. (**a**) HeLa cells were first transfected with GFP plasmid alone as a control or with GFP-SHIP2. 24 h later, cells were treated with vehicle or SHIP2 inhibitor for 24 h then followed by 1 mM H_2O_2 for 1 h. Cells were than fixed and mounted. Scale bar: 10 μM. (**b**) HeLa cells were treated with a vehicle or AS19 for 24 h subsequently followed by AKT activator (SC79), 20 μM for 2 h and 1 mM H_2O_2 for 4 h. Total lysates were analysed for the indicated antibodies.

Figure S4.

SHIP2 inhibition enhances PI (4,5)P2 accumulation. HeLa cells were first transfected with plasmid GFP-tagged PLCδ-PH domain, 6 h later they were treated with vehicle or AS19 for 24 h, then fixed and mounted. Fluorescent images of PI (4,5) P2 levels are shown. (C-) vehicle treated cells. Scale bar: 10 μM.

Figure 1

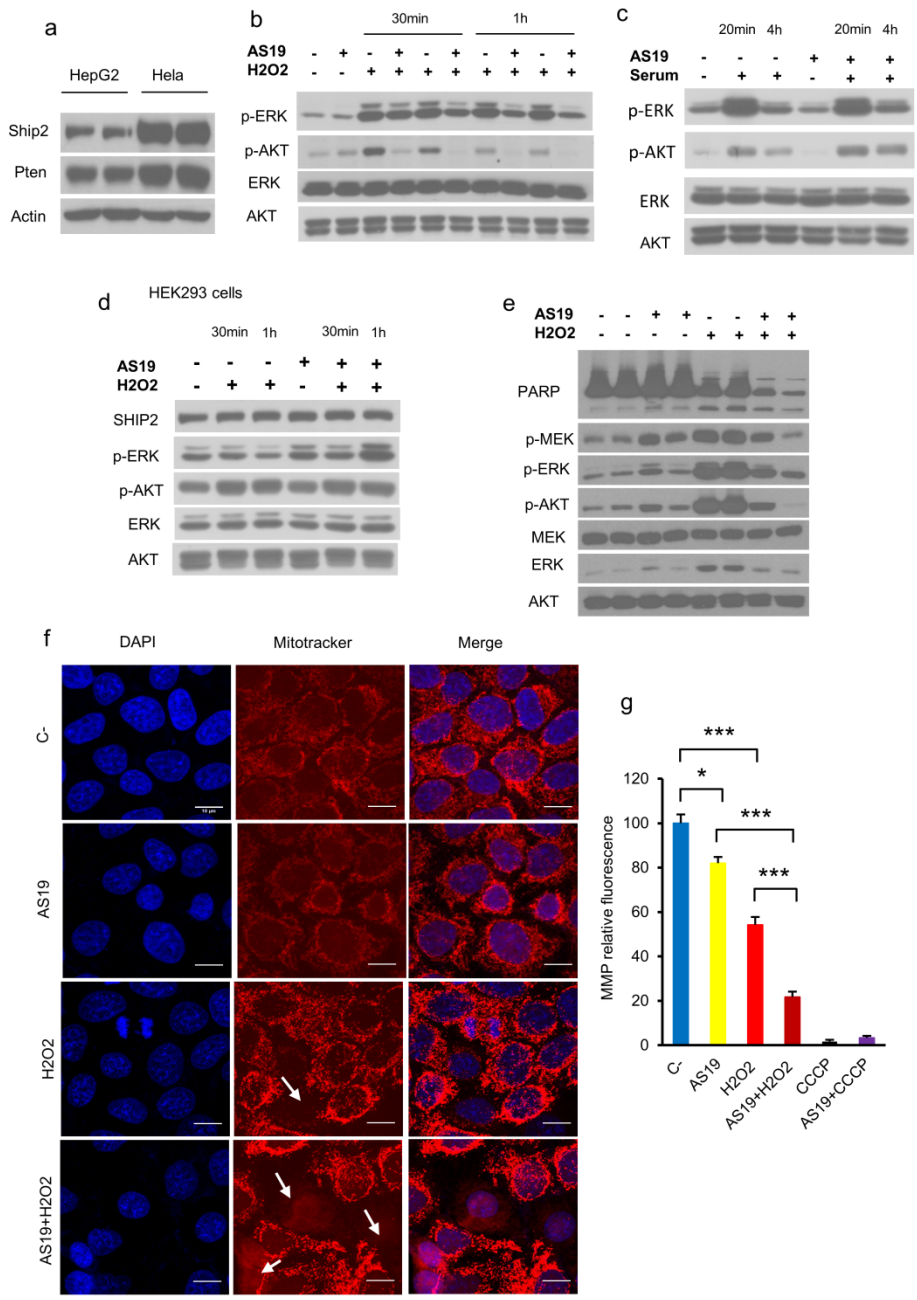

feb4_12967_f1.tif

Figure 2

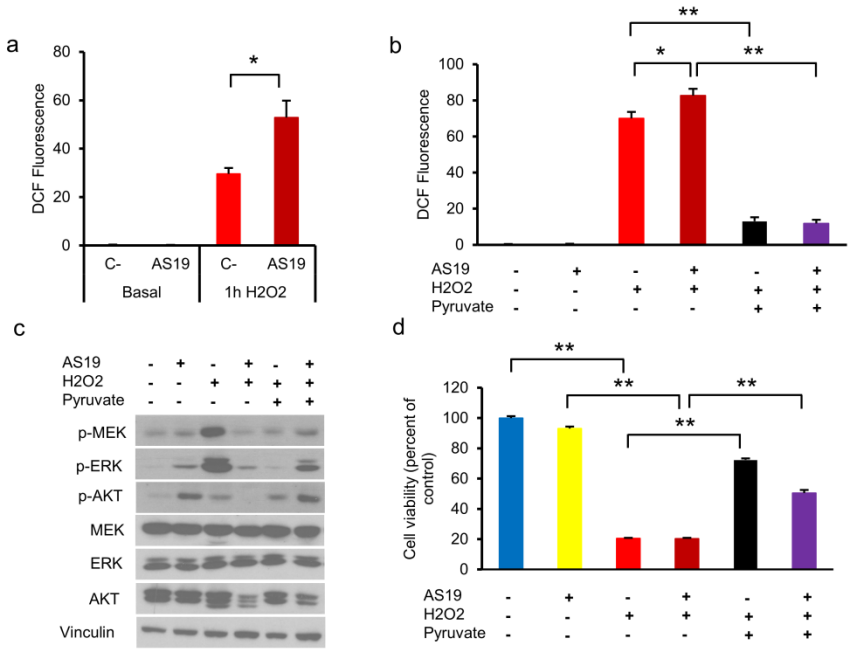

feb4_12967_f2.tif

Figure 3

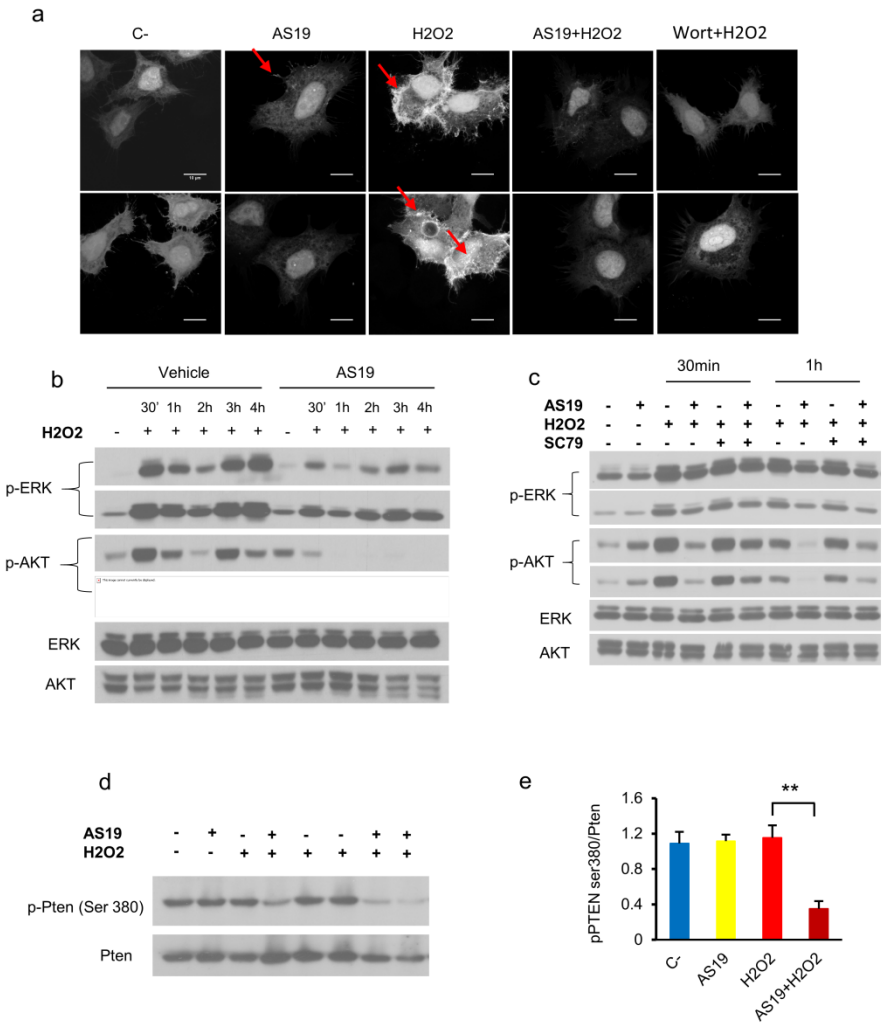

feb4_12967_f3.tif

Figure 4

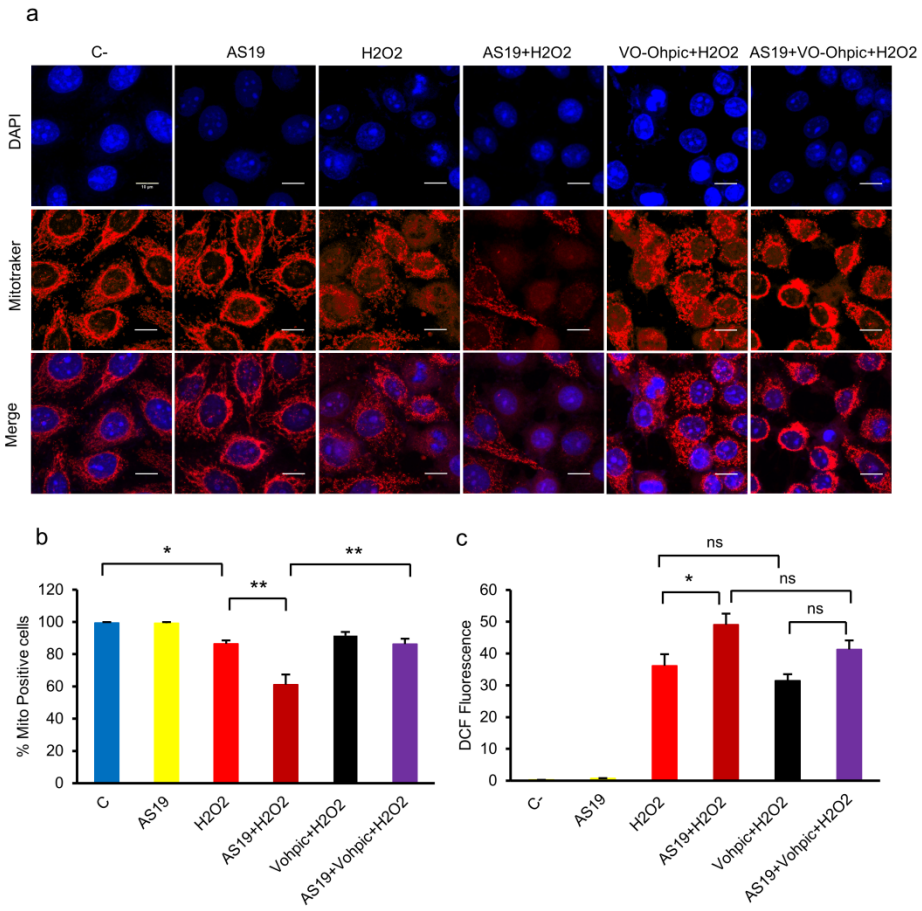

feb4_12967_f4.tif

Figure 5

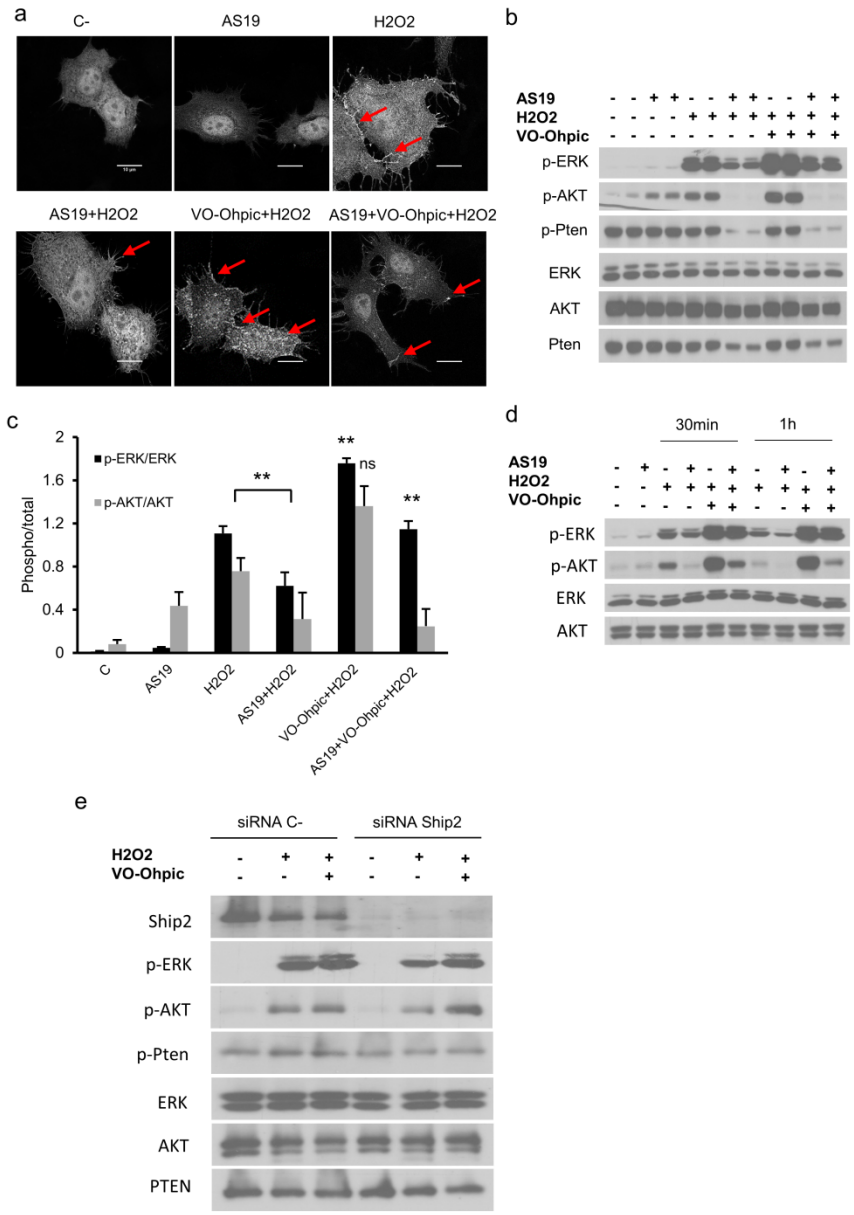

feb4_12967_f5.tif

Figure 6

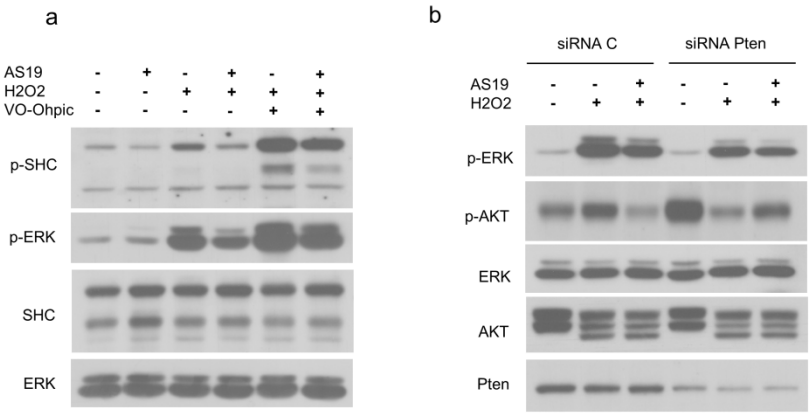

feb4_12967_f6.tif